IJRCS

International Journal of Robotics and Control Systems
Vol. 5, No. 5, 2025, pp. 2568-2588
ISSN 2775-2658
http://pubs2.ascee.org/index.php/ijrcs

ASCEE

Tracking Trajectories of a Quad-Rotor Using Output-Linear Regulator with Hybrid Exosystem, Dwell-Time Analysis

Fernando Castrejón-Rafaela [a,1], Jesús-Alberto Meda-Campaña [b,2], Ricardo Tapia-Herrera [c,3], Jonathan-Omega Escobedo-Alva [a,4,*]

[a] SEPI ESIME Ticomán, Instituto Politécnico Nacional, Mexico
[b] SEPI ESIME Zacatenco, Instituto Politécnico Nacional, Mexico
[b] SECIHTI-SEPI ESIME Zacatenco, Instituto Politécnico Nacional, Mexico
[1] fcastrejonr1700@alumno.ipn.mx; [2] jmedac@ipn.mx; [3] rtapiah@ipn.mx; [3] jescobedoa@ipn.mx
* Corresponding Author

ARTICLE INFO

Article history
Received May 15, 2025
Revised September 06, 2025
Accepted November 21, 2025

Keywords
Bézier Curves;
Dwell Time;
Hybrid Systems;
Output Linear Regulator;
Quadrotor Control;
Tracking

ABSTRACT

The objective of this work is to obtain an algorithm that defines an affordable trajectory in order to cover any points in space in function of dynamics capabilities of a quadrotor. Using the exosystem concept of output linear regulation, an inverse methodology was implemented, that goes from the required points, to Bézier curves and finally, to the differential equation of the exosystem. The condition for the existence of the solution of Francis equation was implemented in order to get a metric to quantify the required time for trajectory tracking in function of the dynamical capabilities of the plant and the maximal initial error. Under the given control framework, tracking performance is primarily influenced by plant dynamics. Moreover, trajectories can be continuously tracked due to the invariance properties of output linear regulators. These results are applicable only on the linear region of plant dynamics.

1. Introduction

There is a growing demand for unmanned aerial vehicles (UAVs), including quadrotor drones. Over time, increasingly complex and powerful algorithms have been developed, significantly enhancing the performance and robustness of drone missions. The control laws governing these systems have achieved near-complete satisfaction regarding performance, stability, fault tolerant and maneuverability, see for example [1]-[14]. However, the inherent dynamics of quadrotors pose challenges for experimental implementation [1], [15]-[17]. Numerous specific problems in this domain continue to evolve, leading to continuous improvements. The growing demand for UAVs and the significance of trajectory tracking can be explained in [2]. A complete research can be found in [3] the author presents the classical PID like an excellent option for small vehicles, due to simplicity and easy tuning. Due to the stability of quadrotor the principal control law used for the quadrotor are the PID controller, see [8], [15], [20]-[26].

For MIMO system the linear quadratic regulator is considered an excellent option, since the A matrix of QUAV (quadrotor like unmanned aerial vehicle) is simple, (see the matrix A of the equation (6) in this paper) and this optimization tool permit an excellent tracking performance. Citing the same

work, when the unpredictability dynamics must be considered in an operational environment, is recommended to use the H_∞ stratagem [4], although if the non-linearities exists in a considerable operational region, the tuning of control will be difficult [5]-[7]. In the published work [3] explains the Model Predictive Control as an advanced control, converting the tracking error problem in the classical optimization problem of minimization. The author presents and compare different options like: Feedback Linearization Control, Backstepping Control [8], Sliding Mode Control, Fuzzy Controller, Model Reference Adaptive controller, L1 Adaptive Controller, Nonlinear Auto Regressive Moving Average L2 Controller. Is highly recommended the discussion and comparative analysis of [3]. An important conclusion is: "Addressing these practical limitations requires careful consideration of system constraints, robust control design, and optimization of computational resources to ensure reliable and efficient operation in real-world environments." [3].

Additionally, the author recommends hybrid or learning-based technologies. With regard to these new strategies, it can be found advanced methodologies in [9], this approach is complex but is a robust solution and gives an efficient control. The published work in [10] presents an UAV application with high precision requirements, using and mixing different optimizer tools to track circular paths. The use of Neural Networks has been used successfully like an optimization tool in many works, see [11]. O an interesting fusion of Backstepping with neural networks can be seen in [12], [13]. An approach with AI methodologies that shows that such algorithms have big potential for plants with complex dynamics can be found in [14].

One such challenge is the trajectory tracking problem for individual drones in specialized missions, such as tracking humans, animals, high-speed vehicles, or military targets in combat scenarios [15]-[17]. Some- times, a predefined trajectory must be followed to track specific objectives [18]. Advanced algorithms typically incorporate obstacle avoidance strategies, making trajectory planning particularly complex due to the unknown dynamic capabilities of the drone in tracking the required path, for obstacle avoidance an AI stratagem is presented in [19], where Bézier curves and Laplacian-based Spline Gradient Flow are used. Various methodologies have been proposed to design well-defined trajectories, such as concatenating different segments and employing discrete dynamics, as seen in [20]. Another widely used approach is differential flatness-based optimal planning, which enables trajectory definition in critical emergency scenarios, an example can be found in [21] and [22], where flight paths are optimized for under-actuated systems.

All stratagems presented above are unbeatable in some aspects. But in accordance to [3] a real system constraint is not considered. In this work the simple theory of output linear regulator theory is used, taking advantage in the invariance properties and the well-defined Francis equations [23]. Taking account, the real system constraints, the initial situation of the QUAV and the desired path; a simple technique like output linear regulator could be efficient and robust. Since the 70's the output linear regulator theory has no the same actual impact like the algorithms presented before. But here is employed like a useful tool for the objectives explained.

In the framework of output linear regulator theory, the internal model principle allows trajectories to be integrated as an exosystem within the entire system, transforming the tracking regulation problem into a strategy as robust as the invariance principle is. Furthermore, the system remains invariant to any initial conditions of both the exosystem and the plant, and its robustness has been extensively validated in previous studies [24]-[26]. Using Bézier curves as a basis for trajectory generation is one of the multiples parametrized curves, is advantageous because it simplifies the exosystem construction, and allows a smooth and continuous transitions through designated way-points in space. This approach has been effectively demonstrated in applications such as [27].

Even though the invariance property is present, several uncertainties remain unresolved. In the state if the art there is currently no rigorous analysis of the specific properties that the quadrotor must exhibit or the limits of the trajectory it should follow most notably, how far the quadrotor can be from the intended path before it starts tracking. Since the trajectory is constructed by piecing together several segments each defined by a differential equation whose solution forms part of the overall path

a hybrid stability analysis is necessary to assess tracking capabilities rigorously. In literature, the simplest form of such analysis involves the concept of "dwell time" [28], [29].

Incorporating the internal model principle, the output linear regulator enables the inclusion of trajectory dynamics as part of the plant. To achieve this, it is necessary to construct the differential equations corresponding to the trajectory to be tracked. A practical approach for defining arbitrary trajectories involves constructing them using segments of third-degree Bézier curves. This differential equation combines discrete changes in initial conditions, effectively transforming the system into a hybrid dynamical model. The continuous and discrete components of the differential equation must be designed to represent the original Bézier curve accurately.

"The main contribution of this work is the use of the "dwell-time" concept in order to know the characteristics necessary to track trajectories in a satisfactory manner, the stratagem consists in substitution of the Francis equation into the solution of the system, obtaining the dwell-time formulation. A numerical example is presented for a quadrotor tracking a 3D complex and closed trajectory." This work is only a theoretical approach, and only intended to gives an initial tool to determine the dynamic capabilities of the quadrotor to follow certain waypoints in function of the initial tracking error. The experimental validation involves many more problems that need to be solved and is proposed as an opportunity for the reader, or as future work for the authors.

2. Method

In accordance to the introduction and the published work [3] in function of the specific tracking problem, a methodology could be superior than others. In general, the output linear regulator with exosystems is not superior, but is a simple way to generate an algorithm in which there is prior knowledge of the exact capabilities of the system to follow a given trajectory. According to the definition of a linear output regulator, the exosystem can be tracked regardless of the initial conditions of both the plant and the exosystem [23]. However, this principle applies only to a single exosystem. In this case, multiple exosystems switch at unknown time instants, necessitating a dedicated analysis of the tracking performance under these conditions. Consequently, it is essential to determine the limitations of the proposed method to ensure its effectiveness in this specific scenario. First a description of the Quadrotor Model is presented, and the basic theory formulation for Linear Output Regulator. The Quadrotor Dynamics are linearized in hover condition, the system is stable with all eigenvalues equal to zero. A simple feedback control can be applied in order to obtain an advantageous asymptotic stability for an easy tracking, the plant will keep yaw motion fixed, and pitch and roll will be used to tridimensional translations.

In next section the methodology for construction of Bézier Curves like Hybrid System is presented. The Bézier curves will conform three-degree polynomials time depending and with three unknown constants to be calculated. The feasibility consists in a parametrized curve that is constructed from two point defining the first and last obligatory pints (points where the quadrotor is required to flight), the other two intermediate points are care of reach continuity and smoothness with the neighboring curves of the global trajectory constructed for the N Bézier curves. The classical Jordan form is applied to construct solution of linear differential equation that is associated to the Bézier curves. Then the structure of the output linear regulator with the differential equation that is associated to the Bézier curves represented like exosystem is presented, using the classic nomenclature for Hybrid Systems. In results section the Bézier curves definition and the Output Linear Regulator theory are merged to construct the exosystems. This exosystem will be introduced in the plant dynamics. Although the plant dynamics with feedback control is asymptotically stable, the exosystem could be unstable. But each exosystem solutions draws only one segment of the trajectory, and therefore it will be switching. This switching signal will be maintaining solution exosystem bounded [30], and the output linear regulator will be capable of reducing error tracking dynamics sufficiently. When this event occurs, the switching signal is called: "dwell time signal" [31]. And Flowchart diagram of the entirely approach is presented in Fig. 1.

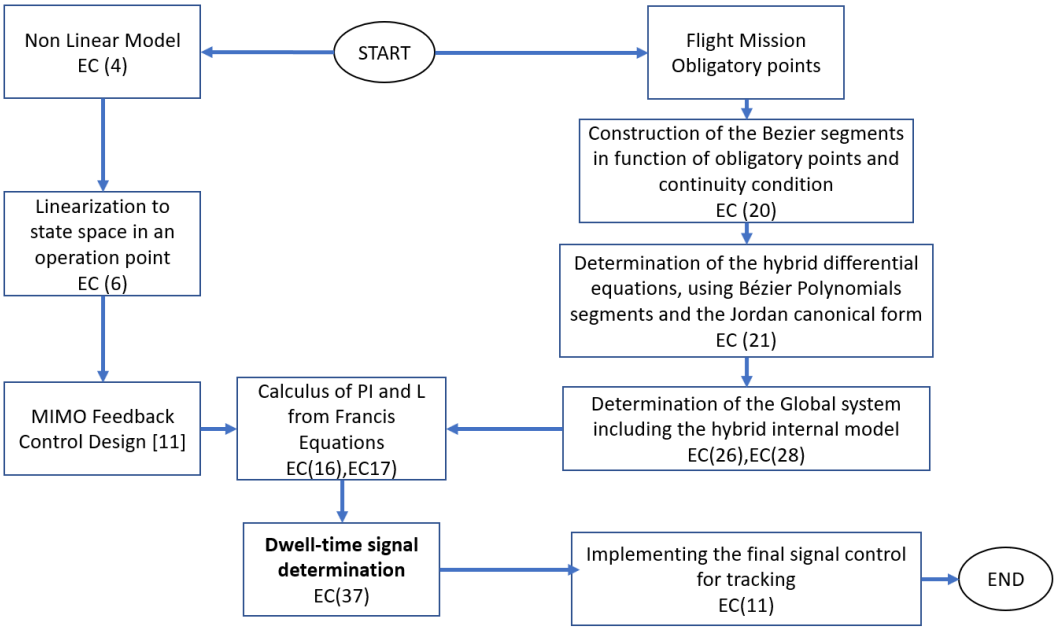

Fig. 1. Methodology flowchart

2.1. Quadrotor Model

In this work a non-linear model of quadrotor was used, in accordance to [32], [33] and [34], the dynamics are expressed like:

$$\dot{x}(t) = f\big(x(t), u(t)\big) \tag{1}$$

$$y(t) = h\big(x(t)\big) \tag{2}$$

The output vector is defined like:

$$h(x) = Cx \tag{3}$$

With $C = I_{12\times12}$, and $I_{12\times12}$ is the identity matrix with a dimension of 12×12.

The state and control are $x(t) = [x1(t)\ldots x12(t)]^T$, $u(t) = [u1(t)\ldots u4(t)]^T$. The equation system in (1) is defined like:

$$\begin{Bmatrix} \dot{x}_1 \\ \dot{x}_2 \\ \dot{x}_3 \\ \dot{x}_4 \\ \dot{x}_5 \\ \dot{x}_6 \\ \dot{x}_7 \\ \dot{x}_8 \\ \dot{x}_9 \\ \dot{x}_{10} \\ \dot{x}_{11} \\ \dot{x}_{12} \end{Bmatrix} = \begin{bmatrix} x_2 \\ \big(sin(x_{11})sin(x_7) + cos(x_{11})sin(x_9)cos(x_7)\big)\dfrac{\beta_1}{m} \\ x_4 \\ \big(-cos(x_{11})sin(x_7) + sin(x_{11})sin(x_9)cos(x_7)\big)\dfrac{\beta_1}{m} \\ x_6 \\ -g + cos(x_9)\,cos(x_7)\dfrac{\beta_1}{m} \\ x_8 \\ x_{10}x_{12}\dfrac{I_{yy}-I_{zz}}{I_{xx}} - \dfrac{J_{tp}}{I_{xx}}x_{10}\Omega + \dfrac{l\beta_2}{I_{xx}} \\ x_{10} \\ x_8x_{12}\dfrac{I_{zz}-I_{xx}}{I_{yy}} - \dfrac{J_{tp}}{I_{yy}}x_8\Omega + \dfrac{l\beta_3}{I_{yy}} \\ x_{12} \\ x_8x_{10}\dfrac{I_{xx}-I_{yy}}{I_{zz}} + \dfrac{l\beta_4}{I_{zz}} \end{bmatrix} \tag{4}$$

Where x_1, x_2, x_3 are the linear displacements in meters along earth axis X_e, Y_e, Z_e respectively, see Fig. 2. A similar model can be found in [35].

The variables x_7, x_9, x_{11} are angular displacements in radians on body axis X_b, Y_b, Z_b. The β inputs are defined.

$$\begin{aligned} \beta_1 &= b(u_1^2 + u_2^2 + u_3^2 + u_4^2), \\ \beta_2 &= b(u_4^2 + u_3^2 - u_1^2 - u_2^2), \\ \beta_3 &= b(u_2^2 + u_3^2 - u_1^2 - u_4^2) \\ \beta_4 &= d(u_1^2 + u_3^2 - u_2^2 - u_4^2), \\ \Omega &= u_1 - u_2 + u_3 - u_4. \end{aligned} \tag{5}$$

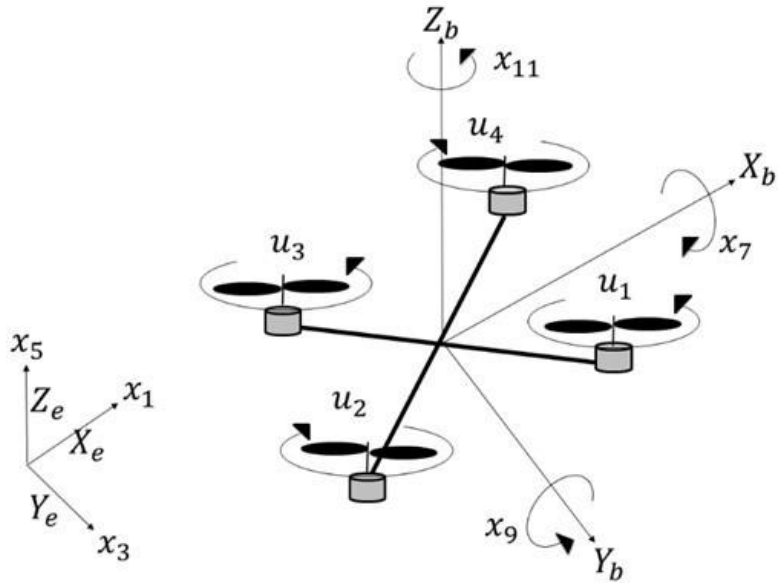

Fig. 2. Quadrotor diagram obtained from [33]

The effective controls are the frequency rotors u_1, u_2, u_3, u_4 in radians per second. The displacement is caused by $\beta_1(t), \beta_2(t)$ causes a roll movement, $\beta_3(t)$ induces pitch and $\beta_4(t)$induces yaw. The parameters shown in (4) and (5) are:

b = 54.2 × 10−6 Ns2,

d = 1.1 × 10−6 Nms2,

l = 0.24 m,

m = 1 kg,

g = 9.81 m/s2,

Jtp = 104 × 10−6 Nms2,

Ixx = 8.1 × 10−3 Nms2,

Iyy = 8.1 × 10−3 Nms2,

Izz = 14.2 × 10−3 ms2.

In an ideal condition, the quadrotor flight will maintain small attitude angles, considering this, we selected hover flight like trim condition. The necessary input for trim condition in hover flight is $u_i(t) = 212.72 \frac{rad}{s}$ with $i = 1, \ldots 4$. The linearized model with trim condition (x_0, u_0) is given for the next equations:

$$\dot{x} = Ax + Bu, \tag{6}$$

$$y = Cx + Du. \tag{7}$$

Where

$$x_0 = [O]_{12\times1}, u_0 = \begin{bmatrix} 212.7183 \\ 212.7183 \\ 212.7183 \\ 212.7183 \end{bmatrix}. \tag{8}$$

In (6) and (7), $A \in R12 \times 12, B \in R12 \times 4, C \in R4 \times 12, D \in R4 \times 4$, all values are zero excepting the next definitions: For matrix A:

A (1, 2) = A (3, 4) = A (5, 6) = A (5, 6) = A (9, 10) = A (11, 12) = 1, A (4, 7) = A (2, 9) = 9.81.

For matrix *B*:

B (6, :) = 0.0231, B (8, :) = −0.6832, B (10, :) = −0.6832, B (12, :) = 0.0330.

For matrix *C*:

$$C(1,1) = C(1,3) = C(3,5) = C(4,11) = 1 \tag{9}$$

2.2. Output Linear Regulator

In accordance to output linear regulation theory, the complete system is conformed for the plant state *x* and the exosystem *w*, the output and error dynamics are presented in (10).

$$\begin{aligned} \dot{x} &= Ax + Bu, \\ \dot{w} &= Sw, \\ y &= Cx + Qw, \\ \varepsilon &= Cx - Qw. \end{aligned} \tag{10}$$

The Q matrix defines the variables of the exosystem to be tracked. The control law in (11) is con- formed for a feedback matrix gain K designed for the stability of the plant and a L matrix to be designed.

$$u = Kx + Lw. \tag{11}$$

For check different control strategies (K gain matrix from equation (11)) in quadrotor see [36]. The new vector state is:

$$x_s = \begin{Bmatrix} x \\ w \end{Bmatrix} \tag{12}$$

And the final system is presented in (13).

$$\begin{aligned} \dot{x}_s &= (A + BK)x + (BL)w, \\ w &= Sw, \\ \varepsilon &= Cx + Qw. \end{aligned} \tag{13}$$

Consider the feedback matrix like $A_1 = A + BK$. As can be seen in the matrix A_s of (14), the control law L will maintain the plant in the span of the exosystem, as long as the K control law is correctly designed for a Hurwtiz matrix $(A + BK)$.

$$A_s = \begin{bmatrix} A + BK & BL \\ 0 & S \end{bmatrix}. \tag{14}$$

In (14) is important to note that the eigenvalues of S are all zero. That is:

$$\bar{\sigma}(S) = 0, \tag{15}$$

With $\bar{\sigma}(\cdot)$ known as spectrum.

The process for the output linear regulator design is clarified for the next lemma: Consider the feedback system in (13) and suppose that $A + BK$ is Hurwitz, then: $\lim_{t\to\infty} \varepsilon(t) = 0$.

For any (x_0, w_0) if and only if (Π, L) from:

$$(A + BK)\Pi - \Pi S = BL, \tag{16}$$

Is such that:

$$-C\Pi + Q = 0. \tag{17}$$

This is a known condition for Output Linear Regulator established for Francis and Wonham in [37].

3. Results and Discussion

3.1. Bézier Curves and Hybrid Exosystem

Given the linear-time-invariant system:

$$\begin{aligned} \dot{w} &= Sw, \\ y_e &= Qw \end{aligned} \tag{18}$$

The solution is

$$w(t) = e^{S(t-t_1)}w(t_1). \tag{19}$$

On the other hand, a parametric third-degree Bézier curve can be defined like: $B(t) = \left(1 - \frac{t-t_1}{t_2-t_1}\right)^3 P_1 + 3\left(\frac{t-t_1}{t_2-t_1}\right)\left(1 - \frac{t-t_1}{t_2-t_1}\right)^2 P_2 + 3\left(\frac{t-t_1}{t_2-t_1}\right)^2\left(1 - \frac{t-t_1}{t_2-t_1}\right)P_3 + \left(\frac{t-t_1}{t_2-t_1}\right)^3 P_4$.

Once this is established, the aim is to emulating $B(t)$ with exosystem output y_e in the elapsed time $t \in [t_1, t_2]$. Suppose that the control points P_i with $i = 1, \ldots, 4$ are known and are defined as uni- dimensional coordinates x, the time-span $t \in [t_1, t_2]$ is also known. Since all parameters in $B(t)$ are well known, the Bézier function could be defined as:

$$B(t) = at^3 + bt^2 + ct + d, \tag{20}$$

With a, b, c, d like coefficients of polynomial. $B(t)$ is a linear combination of coordinates and time instants t_1, t_2.

As mentioned in the last section this solution of exosystem $w(t)$ shall equal than Bézier curve. $B(t)$. This is possible using a general solution for an exosystem using the Jordan form and setting with the polynomial; $w(t) = B(t)$.

First the solution in the Jordan form can be obtained with the classical next transformation, see for example [28], $J = PSP^{-1} = \begin{bmatrix} J_1 & 0 & \cdots & 0 \\ 0 & J_2 & \cdots & 0 \\ \vdots & \vdots & \ddots & \vdots \\ 0 & 0 & \cdots & J_l \end{bmatrix}$.

With a total of l Jordan blocks. Each of the J_i block has the next form: $J_i = \begin{bmatrix} \lambda_i & 1 & \cdots & 0 \\ 0 & \lambda_i & \cdots & 0 \\ \vdots & \vdots & \ddots & \vdots \\ 0 & 0 & \cdots & \lambda_i \end{bmatrix}_{n_i \times n_i}$

Wach λ_i is an eigenvalue of S, the matrix P contains the eigenvector of S. From the normal Jordan a simpler solution of e^{St} can be presented:

$$e^{St} = P^{-1}\begin{bmatrix} e^{J_1 t} & 0 & \cdots & 0 \\ 0 & e^{J_2 t} & \cdots & 0 \\ \vdots & \vdots & \ddots & \vdots \\ 0 & 0 & \cdots & e^{J_l t} \end{bmatrix} P, e^{J_i t} = e^{\lambda_i t}\begin{bmatrix} 1 & t & \frac{t^2}{2!} & \cdots & \frac{t^{n_i-1}}{(n_i-1)!} \\ 0 & 1 & t & \cdots & \frac{t^{n_i-2}}{(n_i-2)!} \\ \vdots & \vdots & \vdots & \ddots & \vdots \\ 0 & 0 & 0 & \cdots & t \\ 0 & 0 & 0 & \cdots & 1 \end{bmatrix}.$$

For the exosystem, it is important to consider the spectrum defined in (15). Furthermore, for a third- degree polynomial, the dimension n is setting to 4. Then the Jordan matrix will be:

$$J = \begin{bmatrix} 0 & 1 & 0 & 0 \\ 0 & 0 & 1 & 0 \\ 0 & 0 & 0 & 1 \\ 0 & 0 & 0 & 0 \end{bmatrix}, e^{Jt} = e^0\begin{bmatrix} 1 & t & \frac{t^2}{2!} & \frac{t^3}{3!} \\ 0 & 1 & t & \frac{t^2}{2!} \\ 0 & 0 & 1 & t \\ 0 & 0 & 0 & 1 \end{bmatrix},$$

With substitution of $t = t - t_1$: $e^{J(t-t_1)} = \begin{bmatrix} 1 & t-t_1 & \frac{(t-t_1)^2}{2} & \frac{(t-t_1)^3}{6} \\ 0 & 1 & t-t_1 & \frac{(t-t_1)^2}{2} \\ 0 & 0 & 1 & t-t_1 \\ 0 & 0 & 0 & 1 \end{bmatrix}$.

The exosystem solution is

$$w(t) = \begin{bmatrix} \frac{w_4(t_1)(t-t_1)^3}{6} + \frac{w_3(t_1)(t-t_1)^3}{2} + w_2(t_1)(t-t_1) + w_1(t_1) \\ \frac{w_4(t_1)(t-t_1)^2}{2} + w_3(t_1)(t-t_1) + w_2(t_1) \\ w_4(t_1)(t-t_1) + w_3(t_1) \\ w_4(t_1) \end{bmatrix}. \quad (21)$$

For observation, the first row of (21), is in the same form than (20) and the next rows are their first, second and third derivative respectively. The evolution of system will be function from initial conditions only.

$$w(t_1) = \begin{bmatrix} w_1(t_1) \\ w_2(t_1) \\ w_3(t_1) \\ w_4(t_1) \end{bmatrix}$$

Replacing $t = t_1$ in (21): $\begin{bmatrix} B(t_1) \\ B'(t_1) \\ B''(t_1) \\ B'''(t_1) \end{bmatrix} = \begin{bmatrix} 1 & t_1 - t_1 & \frac{(t_1-t_1)^2}{2} & \frac{(t_1-t_1)^3}{6} \\ 0 & 1 & t_1 - t_1 & \frac{(t_1-t_1)^2}{2} \\ 0 & 0 & 1 & t_1 - t_1 \\ 0 & 0 & 0 & 1 \end{bmatrix}\begin{bmatrix} w_1(t_1) \\ w_2(t_1) \\ w_3(t_1) \\ w_4(t_1) \end{bmatrix}$,

For calculus of initial conditions, we obtain an identity matrix and we have the next important result:

$$w(t_1) = \begin{bmatrix} B(t_1) \\ B'(t_1) \\ B''(t_1) \\ B'''(t_1) \end{bmatrix}. \quad (22)$$

That's mean that the exosystem differential equation presents the initial condition t_1 defined for the Bezier curve and their derivatives in the instant t_1. For error equation of the corresponding variables the output exosystem is defined like:

$$y_e(t) = Qw(t). \tag{23}$$

For a three-dimensional space the equation (18) and the Q 12×12 dimensional matrix becomes to:

$$Q = \begin{bmatrix} 1 & 0 & 0 & 0 & 0 & 0 & 0 & 0 & 0 & 0 & 0 & 0 & 0 & 0 & 0 & 0 \\ 0 & 0 & 0 & 0 & 1 & 0 & 0 & 0 & 0 & 0 & 0 & 0 & 0 & 0 & 0 & 0 \\ 0 & 0 & 0 & 0 & 0 & 0 & 0 & 0 & 1 & 0 & 0 & 0 & 0 & 0 & 0 & 0 \\ 0 & 0 & 0 & 0 & 0 & 0 & 0 & 0 & 0 & 0 & 0 & 0 & 1 & 0 & 0 & 0 \end{bmatrix} \tag{24}$$

The equations (23) and (24) with initial condition defined as (22) conforms the exosystem that defines the trajectories passing through the points presented in (19). The S matrix which define the dynamics of the exosystem $\dot{w}(t) = Sw(t)$, is a 12×12 superdiagonal matrix of ones for each dimensional variable and each trajectory segment, the form of the trajectory is defined only by the initial conditions.

3.2. Output Linear Regulator with Hybrid Exosystem

In accordance to the hybrid nomenclature in [29] and [31], the hybrid system is defined by $H = \{F, G, C, D\}$ the hybrid state variable z is the vector:

$$z = \begin{Bmatrix} x_s \\ w \\ \tau \end{Bmatrix}. \tag{25}$$

The continuous dynamics $F(z)$ is defined by

$$F(z) = \begin{cases} \dot{x}_s = (A + BK)x + BLw, \\ \dot{w} = Sw, \\ \dot{\tau} = \dfrac{1}{t_{j+1} - t_j}, \end{cases} \tag{26}$$

With the flow map:

$$\mathcal{C} = \mathbb{R}^n \times \mathbb{R}^r \times [0,1) \times \mathbb{R}^q. \tag{27}$$

The discrete-time dynamical system is:

$$G(z) = \begin{cases} w^+ = w_{0_j}, \\ \tau^+ = 0 \end{cases} \tag{28}$$

With the jump map:

$$\mathcal{D} = \mathbb{R}^n \times \mathbb{R}^r \times \{1\} \times \mathbb{R}^q. \tag{29}$$

The hybrid domain is defined by:

$$E = \bigcup_{j=0}^{s} ([t_j, t_{j+1}, j]), \tag{30}$$

That's means that the state x_s and exosystem w are continuous in $[t_j, t_{j+1}]$ and the error equation is segmented onto hybrid domains with the next nomenclature:

$$e(t_j, j) = Cx(t_j, j) - Qw(t_j, j). \tag{31}$$

3.2.1. Dwell-Time Signal

To achieve tracking, the error dynamics is no necessary to be stable nor asymptotically stable, the relaxed requirement is a sufficient convergence to an acceptable error in function to flight mission. The next definition is extracted from [31]. σ is a dwell-time signal and the solution is a dwell-time solution with dwell time $\tau_D > 0$ if $t_j + 1 - t_j \leq \tau_D$ for $j = 1, 2$. That is, jumps are separated by at

Least τ_D amount of time. Next, we need to obtain the amount of time τ_D for this special case. The solution of first equation in (26) is established like:

$$x(t,j) = e^{A_1\left(t-t_{0_j}\right)}x_{0_j} + e^{A_1 t}\int_{t_{0_j}}^{t} e^{-A_1\tau}BLw(\tau,j)d\tau,\ A_1 = A + BK.$$

With:

$$w(\tau,j) = e^{S\left(t-t_{0_j}\right)}w_{0_j} - A_1\Pi + \Pi S = BL, \tag{32}$$

Fom solution of complete information problem: $C\Pi = \mathrm{Q}$,

Therefore $x(t,j) = e^{A_1\left(t-t_{0_j}\right)}x_{0_j} + e^{A_1 t}\int_{t_{0_j}}^{t} e^{-A_1\tau}(-A_1\Pi + \Pi S)e^{S\tau}e^{-St_{0_j}}w_{0_j}\,d\tau$,

Knowing that: $\frac{d}{d\tau}[e^{-A_1\tau}\Pi e^{S\tau}] = e^{-A_1\tau}A_1\Pi e^{S\tau} + e^{-A_1\tau}\Pi S e^{S\tau} = e^{-A_1\tau}(-A_1\Pi + \Pi S)e^{S\tau}$,

The following is reached: $x(t,j) = e^{A_1\left(t-t_{0_j}\right)}x_{0_j} + e^{A_1 t}\int_{t_{0_j}}^{t}\frac{d}{d\tau}[e^{-A_1\tau}\Pi e^{S\tau}]d\tau e^{-St_{0_j}}w_{0_j}\,d\tau$,

Finally, solving and reordering results:

$$x(t,j) = e^{A_1\left(t-t_{0_j}\right)}\left(x_{0_j} - \Pi w_{0_j}\right) + \Pi e^{S\left(t-t_{0_j}\right)}w_{0_j}. \tag{33}$$

Consequently, the error solution is obtained substituting in the second Francis equation presented in Lemma 1.

$$\varepsilon(t,j) = Ce^{A_1\left(t-t_{0_j}\right)}\left(x_{0_j} - \Pi w_{0_j}\right) + C\Pi e^{S\left(t-t_{0_j}\right)}w_{0_j} - C\Pi e^{S\left(t-t_{0_j}\right)}w_{0_j}. \tag{34}$$

This result is concluding, is evident than the error dynamics depends only of plant dynamics and Π. In order to reach a specific final error, this equation can be presented like:

$$\varepsilon(t,j) = Ce^{A_1\left(t-t_{0_j}\right)}\varepsilon_{0_j}, \tag{35}$$

Where.

$$\varepsilon_{0_j} = x_{0_j} - \Pi w_{0_j} \tag{36}$$

The error is 3-dimensional vector, therefor the Euclidian norm will be used. Since we can write the error in the next form: $\|\varepsilon(t,j)\| = \left\|Ce^{A_1\left(t-t_{0_j}\right)}\varepsilon_{0_j}\right\| \leq \left\|Ce^{A_1\left(t-t_{0_j}\right)}\right\|\left\|\varepsilon_{0_j}\right\| \leq \|C\|\left\|e^{A_1\left(t-t_{0_j}\right)}\right\|\left\|\varepsilon_{0_j}\right\|$.

Consider the Jordan normal form: $e^{A_1\left(t-t_{0_j}\right)} = e^{P^{-1}J_1\left(t-t_{0_j}\right)P}$,

Where J_1 es the unique Jordan normal form, and T the corresponding eigenvectors. For quadrotor dynamics, the eigenvalues are presented with multiplicity equal to 1, simplifying this analysis. Substituting the normal form in the Euclidian norms: $\|\varepsilon(t,j)\| = \|C\| \left\| e^{A_1\left(t-t_{0_j}\right)} \right\| \left\| \varepsilon_{0_j} \right\| = \|C\| \left\| e^{P^{-1}J_1\left(t-t_{0_j}\right)P} \right\| \left\| \varepsilon_{0_j} \right\|$,

And we can write: $\left\| e^{A_1\left(t-t_{0_j}\right)} \right\| \leq e^{-\alpha\left(t-t_{0_j}\right)}$

Where $\alpha = min\{(Re(|\lambda|) : \lambda \in \sigma^{-}(A1)\}$, that means; the dominant eigenvalue in a Hurwitz matrix. This inequality is trivial and not proof is necessary. See for example [28] for reference. The classical solution for a Linear system can be expressed like: $\|\varepsilon(t,j)\| \leq Ce^{-\alpha\left(t-t_{0_j}\right)} \left\| \varepsilon_{0_j} \right\|$.

With an algebraic process the time necessary to obtain a determined error defined by ε_{s_j} for each jump j is:

$$\tau_{D_j} \geq \alpha^{-1}\left[Ln\left(\frac{\left\|\varepsilon_{s_j}\right\|}{e^{\alpha t_{j-1}}\left\|\varepsilon_{j-1}\right\|}\right)\right] + 1. \tag{37}$$

In (37), ε_{j-1} is the initial error in the jump j, and ε_{s_j} is chosen by performance requirements. Therefore, the τ_{D_j} for each jump j expressed in the Definition 3.1.1 and has been determined.

3.3. Numerical Example

Initial condition for plant is defined like: $x_{0_1} = [9 \quad 0 \quad 7 \quad 0 \quad -1 \quad 0_{1\times 5} \quad 1 \quad 0]^T$. The parametrized curves, like Bézier curves, are interpolations between points that conforms a convex group; these points can be separated like reglementary and construction points, see for example [38]. The "reglementary points" defined bellow does reference to the waypoints through which the quadrotor must fly, and the construction point defines the convexity of the curves, please refer to [38].

The trajectory is defined by the next parameters:

1. Reglementary points number: 5
2. Reglementary points coordinates:

$$P_1 = \begin{Bmatrix} 5 \\ 3 \\ 1 \end{Bmatrix}, P_2 = \begin{Bmatrix} 5 \\ 3 \\ 6 \end{Bmatrix}, P_3 = \begin{Bmatrix} 0 \\ -10 \\ 0 \end{Bmatrix}, P_4 = \begin{Bmatrix} 9 \\ 1 \\ 5 \end{Bmatrix}, P_5 = \begin{Bmatrix} 5 \\ 3 \\ 1 \end{Bmatrix}.$$

3. First segment construction points coordinate:

$$P_{C11} = \begin{Bmatrix} 1 \\ 2 \\ 2 \end{Bmatrix}, P_{C12} = \begin{Bmatrix} 1 \\ 6 \\ 3 \end{Bmatrix}.$$

4. Intermediate segment construction points coordinate:

$$P_{C22} = \begin{Bmatrix} 10 \\ -10 \\ 10 \end{Bmatrix}, P_{C32} = \begin{Bmatrix} 6 \\ 4 \\ 3 \end{Bmatrix}.$$

5. Segments time length (seconds):

$$s_1 \in (0,20), s_2 \in (20,50), s_3 \in (50,90), s_4 \in (90,120).$$

The segments of the Bézier curves defined above are plotted in Fig. 3.

Now, for exosystem construction the initial conditions $w(t_j)$ with $j = 1, 2, 3, 4$ are calculated by the equation (19) as in (22). For a three-dimensional space and the yaw angle constant to zero we obtain the next results.

$$\text{For } j = 1\ (t = 0): x(0) = \begin{bmatrix} 5 \\ -3/5 \\ 3/50 \\ 0 \end{bmatrix}, y(0) = \begin{bmatrix} 5 \\ -3/20 \\ 3/40 \\ -9/1000 \end{bmatrix}, z(0) = \begin{bmatrix} 5 \\ 3/20 \\ 0 \\ 3/1000 \end{bmatrix}, \theta(0) = \begin{bmatrix} 0 \\ 0 \\ 0 \\ 0 \end{bmatrix}.$$

$$\text{For } j = 2\ (t = 20): x(20) = \begin{bmatrix} 5 \\ 3/5 \\ -7/150 \\ -1/2250 \end{bmatrix}, y(20) = \begin{bmatrix} 3 \\ -9/20 \\ -2/75 \\ 1/360 \end{bmatrix}, z(20) = \begin{bmatrix} 6 \\ 9/20 \\ -1/30 \\ -1/1000 \end{bmatrix}, \theta(20) = \begin{bmatrix} 0 \\ 0 \\ 0 \\ 0 \end{bmatrix}.$$

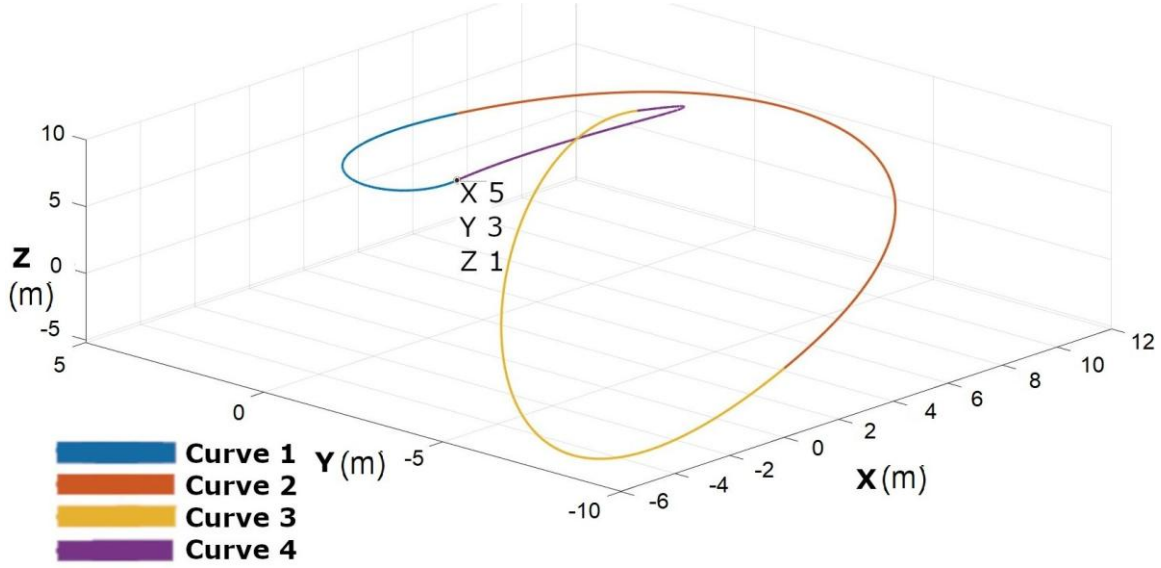

Fig. 3. Three-dimensional trajectory

$$\text{For } j = 3\ (t = 50):$$

$$x(50) = \begin{bmatrix} 0 \\ -1 \\ 49/400 \\ -147/32000 \end{bmatrix}, y(50) = \begin{bmatrix} -10 \\ 0 \\ 21/400 \\ -35/12043 \end{bmatrix}, z(50) = \begin{bmatrix} 0 \\ -1 \\ 89/800 \\ -33/8000 \end{bmatrix}, \theta(50) = \begin{bmatrix} 0 \\ 0 \\ 0 \\ 0 \end{bmatrix}.$$

$$\text{For } j = 4\ (t = 90):$$

$$x(90) = \begin{bmatrix} 9 \\ 9/40 \\ -1/60 \\ -147/32000 \end{bmatrix}, y(90) = \begin{bmatrix} -10 \\ 0 \\ 21/400 \\ -35/12043 \end{bmatrix}, z(90) = \begin{bmatrix} 0 \\ -1 \\ 89/800 \\ -33/8000 \end{bmatrix}, \theta(90) = \begin{bmatrix} 0 \\ 0 \\ 0 \\ 0 \end{bmatrix}.$$

The initial condition w_{0j}

$$w_{0_1} = [x(0)\ y(0)\ z(0)\ \theta(0)]^T,$$
$$w_{0_2} = [x(20)\ y(20)\ z(20)\ \theta(20)]^T,$$
$$w_{0_3} = [x(50)\ y(50)\ z(50)\ \theta(50)]^T,$$
$$w_{0_4} = [x(90)\ y(90)\ z(90)\ \theta(90)]^T.$$

The matrix Q, that is the correlation between plant state and exosystem is a matrix of dimension 4×16, with all values zero excepting: $Q(1,1) = Q(2,5) = Q(3,9) = Q(4,13) = 1$, The exosystem $\dot{w} = Sw$ is defined by:

$$S = \begin{bmatrix} S_0 & 0_{4\times4} & 0_{4\times4} & 0_{4\times4} \\ 0_{4\times4} & S_0 & 0_{4\times4} & 0_{4\times4} \\ 0_{4\times4} & 0_{4\times4} & S_0 & 0_{4\times4} \\ 0_{4\times4} & 0_{4\times4} & 0_{4\times4} & S_0 \end{bmatrix} w(t),\ S_0 = \begin{bmatrix} 0 & 1 & 0 & 0 \\ 0 & 0 & 1 & 0 \\ 0 & 0 & 0 & 1 \\ 0 & 0 & 0 & 0 \end{bmatrix}.$$

With simple pole location design and solving the Francis equations in (16) and (17), the control law $u = -Kx + Lw$, is defined by the next matrices.

$$K = \begin{bmatrix} 39.0817 & 39.8065 & 42.7301 & 35.3146 \\ 50.7845 & 49.7273 & 57.8765 & 41.7761 \\ 65.4254 & 27.7942 & 64.3418 & 25.3095 \\ 111.4329 & 40.8647 & 107.4407 & 35.2827 \\ 148.8666 & 163.8057 & 148.5659 & 163.3193 \\ 82.9342 & 87.2892 & 82.8536 & 87.1599 \\ -452.5554 & -138.0551 & -421.3001 & -101.7553 \\ -53.1071 & -15.0293 & -44.5734 & -6.0062 \\ 175.7201 & 174.1363 & 216.7686 & 130.5047 \\ 16.2599 & 20.3300 & 25.6557 & 10.6795 \\ 16.2599 & -74.5068 & 40.2456 & -74.6869 \\ 42.1137 & -51.1640 & 41.9879 & -51.2434 \end{bmatrix}^T.$$

For Π matrix all values are zero excepting the next: $\Pi(1,1) = \Pi(2,3) = \Pi(3,5) = \Pi(4,6) = \Pi(5,9) = \Pi(6,10) = \Pi(11,13) = \Pi(12,4) = 1, -\Pi(7,7) = -\Pi(8,8) = \Pi(9,3) = \Pi(10,4) = 0.1019, \Pi(7,7) = \Pi(8,8) = -0.1019,$

And for L, the matrix Γ is zero excepting the next terms: $\Gamma(1,11) = \Gamma(2,11) = \Gamma(3,11) = \Gamma(4,11) = 10.8419, -\Gamma(2,15) = -\Gamma(4,15) = \Gamma(1,15) = \Gamma(3,15) = 7.5858,$

And $L = \Gamma + K\Pi$.

For the discrete part of dynamics $G(z)$, the timer τ^+switches the initial conditions $w^+ = w_0$. At the end of a complete closed trajectory (the four segments), the quadrotor will hover at the first point. The Fig. 4, Fig. 5, Fig. 6 shows the tracking error using the linear model of the quadrotor.

The error dynamics is too sensitive to numerical errors, presenting overshooting see Fig. 7, for Simulink simulation is impossible to achieve the exact precision in the switching signal, and this problem can be reduced with a minor elapsed time integration in simulation.

The same linear output regulator was applied to the non-linear system of the quadrotor presenting almost the same performance, at least with a small error initial condition, this can be seen in Fig. 7. The timer is obtained like discrete differential equation as in (38) and (39).

$$\dot{\tau} = \frac{0.01}{t_{j+1} - t_j} \in [0,0.01], \tag{38}$$

$$\tau^+ = 0. \tag{39}$$

The evolution of the signal τ is presented in Fig. 8.

3.4. Dwell-Time

The dwell time of each jump can be obtained with equation (37). The minimal eigenvalue is $\alpha = -1$. The permissible error is chosen like $\varepsilon_{s_i} = 0.01$ for all j. For $j = 1$, the initial error con be calculated with (35). And the norm is $\|\varepsilon_{0_1}\| = 6.083$. The dwell time for $j = 1$ is:

$$\tau_{D_1} \geq \left[Ln\left(\frac{0.01}{e^{-0}\|6.083\|}\right)\right] = 7.4107\ s. \tag{40}$$

For $j = 2, \tau_{D_2} \geq 32.9361\ s, ||\varepsilon(32.9361)|| = 3.601e - 5.$

For $j = 3, \tau_{D_3} \geq 58.3482\ s.$

For $j = 4, \tau_{D_4} \geq 95.9947\ s.$

From $j = 3$ to 4 the error norm is to small, and is not presented.

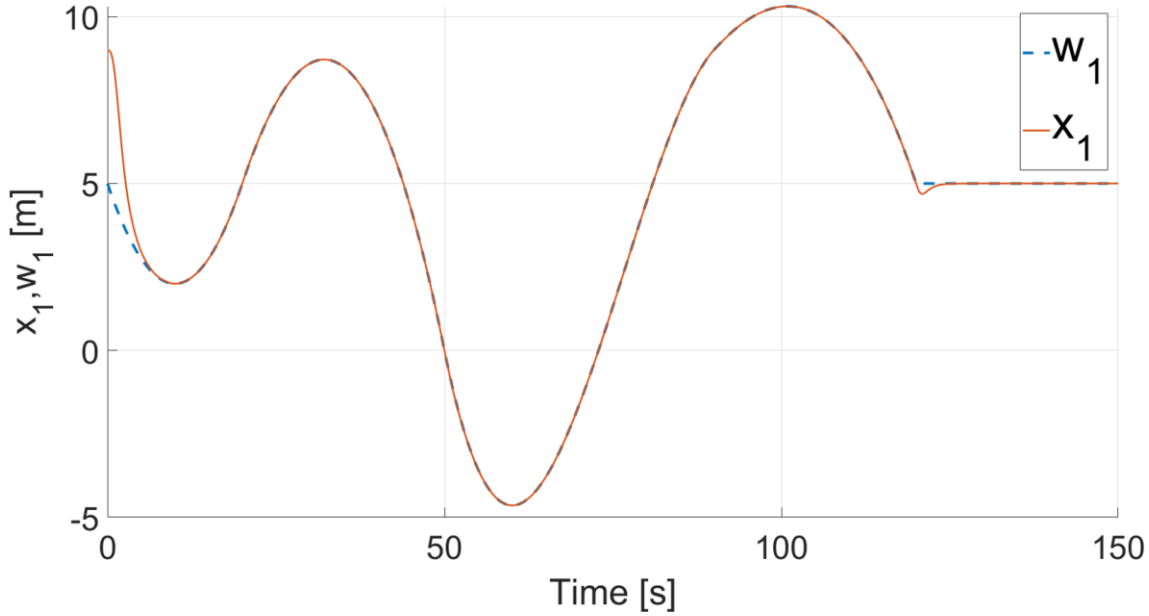

Fig. 4. Exosystem tracking in x-coordinate, earth system, with quadrotor non-linear model

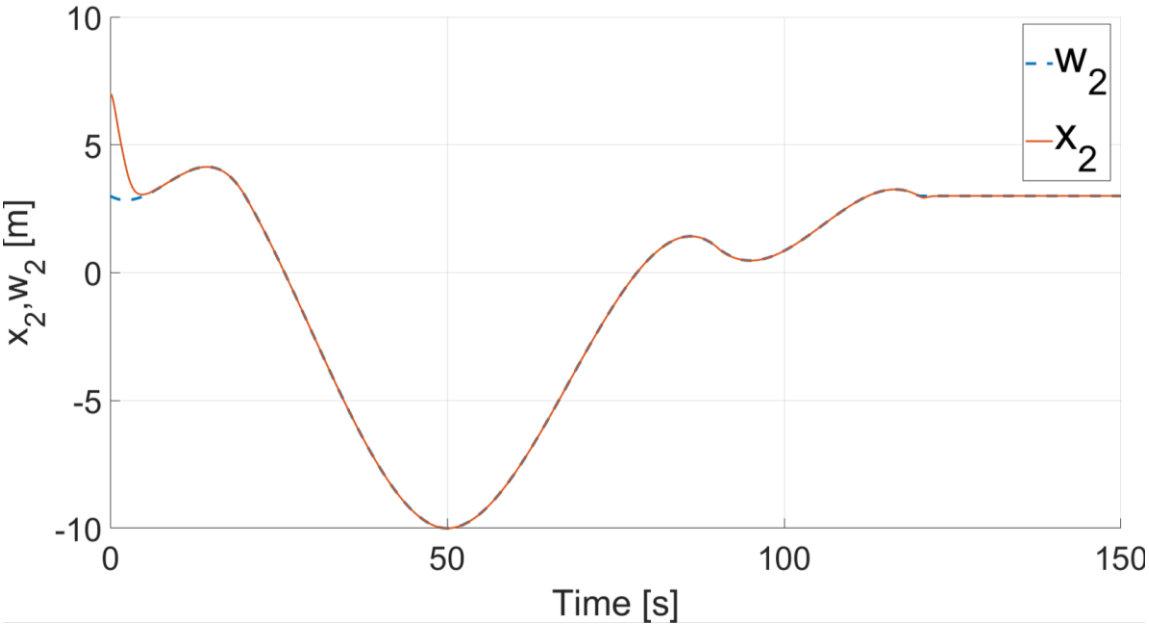

Fig. 5. Exosystem tracking in x-coordinate, earth system, with quadrotor non-linear model

In the next table different initial errors are testing until the output linear regulator fails to track the trajectory. Only the first jump is considered (tracking of the first Bézier curve [34]). This initial error will be obtained with the different positions of the quadrotor.

Due to non-linearities that can be presented in high attitude angles the results on the nonlinear model are also presented. In the last experiment with an initial error of 913.5 m the electric motors are saturated in the maximum operation rate (1100 rad/s or 10,504 rpm), see [34] for operation parameters.

Any initial error greater than 913.5 m fail to track the first segment with a final error of 0.01m, as the presented in the numerical example, check the Fig. 2 and coordinates for the second mandatory points. That's mean, the jumping signal, is not a dwell-time signal.

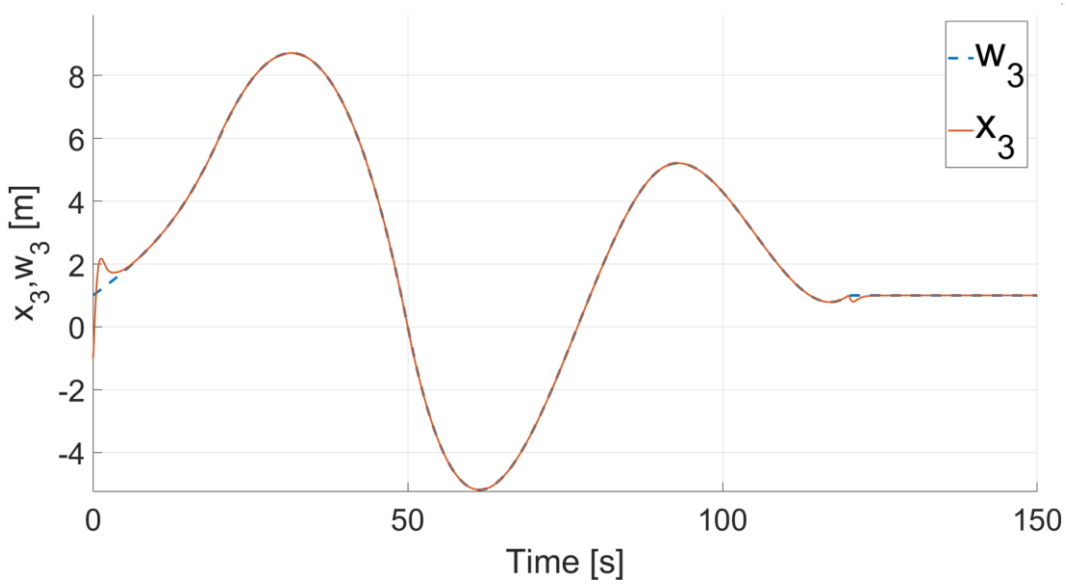

Fig. 6. Exosystem tracking in x-coordinate, earth system, with quadrotor non-linear model

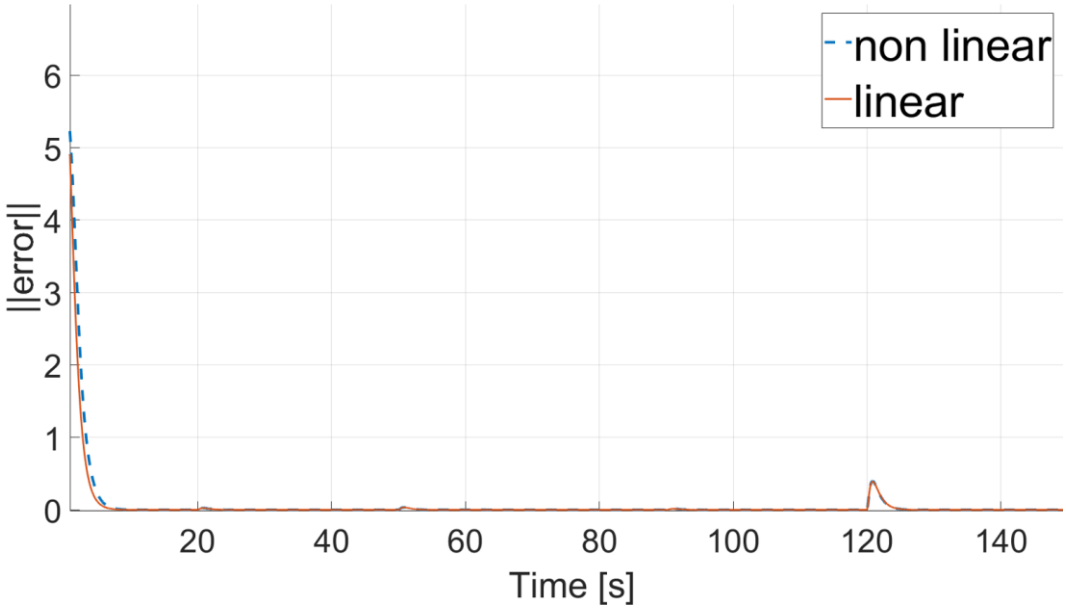

Fig. 7. Tracking error comparison, linear and non-linear quadrotor dynamics

3.5. Discussion

The main calculous involved is the determination of Γ gain matrix through the solution of the Francis equation, as were presented in (16) and (17). This matrix is solved using the "solve" MATLAB Function. In accordance to regulation theory only one Γ gain matrix is applicable to any initial condition, and any trajectory [39]-[45], since only one calculus is necessary for each system (plant dynamics including feedback control), no matters the trajectory problem. For the numerical example presented above, the process takes 7 seconds with a processor Intel(R) Xeon(R) CPU E5-1603 v3 @ 2.80GHz.

In the numerical examples the permissible tracking error was chosen like $0.001\ m$ in all study cases. The quadrotor dynamics is parametrized only by the minimal eigenvalue $\alpha = -1$. The main

contribution in this work is the equation (35), this equation defines the elapsed time necessary for get the permissible tracking error in function on the initial error (distance from quadrotor to desired trajectory), is not trivial as the trajectory are constructed like an exosystem hybrid. The metric is applicable in any segment of the complete trajectory. The construction form Bézier curves permits the inclusion of mandatory points for the quadrotor mission. This stratagem for tracking trajectories not pretends to be better than other existing methods, but gives a tool to determine the dynamical capacities of the plant and any possible trajectory. For more info on different approaches, please refer to [3], [46]-[50].

In order to ensuring stable transition between trajectory segments, the Bezier curves and therefore the exosystem must be smooth and continuous; the invariant principle guarantees the stability of error dynamics as long as the switching signal is a dwell-time switching signal. The results presented here do not included the performance analysis of the regulation theory for tracking trajectory, but the dwell time determination and the theoretical validation using simulations. The experimental validations go beyond the scope of this prelaminar analysis. For an experimental validation the quadrotor and the feedback control shall be correctly identified, the low noise in the actual quadrotor and the electronic system could be simplify the data collection and the applicability of the feedback control and the output linear regulator. Its highly recommended to realize indoor experiments, using a continuous tracking of the quadrotor coordinates, for example using optical devices instead of accelerometers and global navigation systems [51]-[56].

The Table 1 and Fig. 7 shows a similar performance of the output linear regulator in the linear and no linear quadrotor model, this in accordance to [39], but only in the linear region, without a rigorous analysis, and with a trial and error test, the maximum initial condition permissible was the 6.083 m, nevertheless the dwell-time analysis is not capable to determine the final error in the non-linear system [57]-[60].

Table 1. Dwell-time comparation between linear a non-linear quadrotor model for different initial error for the first jump ($j = 1$)

Initial error norm	τ_{D_1}	Arriving time to desired error. Linear System	Final error norm. Linear System	Final error norm. Non-Linear System
6.083 m	7.4107 s	7.4105 s	0.01028 m	0.02244 m
10.1 m	7.92 s	7.92 s	0.0117 m	fail
17.41 m	8.4622 s	8.4602 s	0.01042 m	fail
86.27 m	10.0627 s	10.0621 s	0.01039 m	fail
913.5 m	12.4225 s	12.42 s	0.0112 m	fail

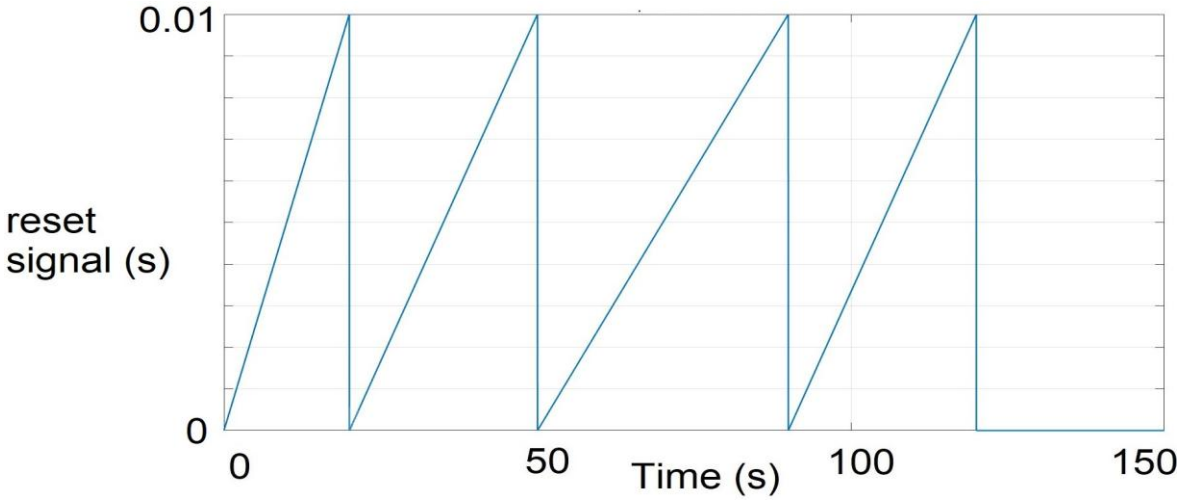

Fig. 8. Timer dynamics

4. Conclusion

This work defines the time required for tracking any trajectory as a function of the initial error and the dynamical properties of a quadrotor with feedback control. Once the first segment is tracked with a minimal error of 0.01 m the next segments will be tracked with no more than 0.01 m error due to invariance properties of an output linear regulator and the insensitive properties of initial conditions of the hybrid exosystem. The analysis of dwell-time shows that, due to the invariance principle, the quadrotor with asymptotic stability will track any well- constructed group of Bézier curves in finite time, no matter the trajectory's complexity or the plant's dynamics with feedback control, due to the way it is built, the Bézier curves permits force the tracking toward the defined points of mission flight. The robustness of the output linear regulators has been proved in many published works, including robustness against noise, external perturbations, and parametric un- certainty, but just theoretically. This analysis is imitated to a small linear region, the dwell-time approach fails to the original non-linear plant. The next recommended step should be and non-linear output regulator and equivalent non-linear dwell time determination. Is obligatory, like future work, an experimental validation of robustness, and linear region limits, and more important for this work, for a dwell-time signal validation, these experiments should be done as recommended in the discussion section.

Author Contribution: All authors contributed equally to the main contributor to this paper. All authors read and approved the final paper.

Funding: This research received not external founding.

Acknowledgment: The partial support provided for this research by the Secretaria de Ciencia, Humanidades, Tecnología e Innovacio´n (SECIHTI) through the SNII (Sistema Nacional de Investigadoras e Investigadores) scholarship. Additionally, the Instituto Politécnico Nacional contributed to this work through research projects [SIP 20250263] and [SIP 20240025], as well as by providing scholarships under the programs EDI (Estímulo al Desempen˜o de los Investigadores), COFAA (Comisio´n de Operacio´n y Fomento de Actividades Académicas), and BEIFI (Beca de Estímulo Institucional de Formacio´n de Investigadores).

Conflicts of Interest: The authors declare no conflict of interest.

References

[1] M. A. Dhaifallah, F. M. Qahtani, S. Elferik, A. W. Saif, "Quadrotor robust fractional-order sliding mode control in unmanned aerial vehicles for eliminating external disturbances," *Aerospace*, vol. 10, no. 8, p. 665, 2023, https://doi.org/10.3390/aerospace10080665.

[2] J. R. S. Benevides, M. A. D. Paiva, P. V. G. Simplício, R. S. Inoue and M. H. Terra, "Disturbance Observer-Based Robust Control of a Quadrotor Subject to Parametric Uncertainties and Wind Disturbance," *IEEE Access*, vol. 10, pp. 7554-7565, 2022, https://doi.org/10.1109/ACCESS.2022.3141939.

[3] A. Fekik *et al*., "Modeling and simulation of quadcopter using self-tuningfuzzy-pi controller," *Mobile Robot: Motion Control and Path Planning*, vol. 1090, pp. 231-251, 2023, https://doi.org/10.1007/978-3-031-26564-8_8.

[4] M. Maaruf, M. S. Mahmoud, A. Ma'arif, "A Survey of Control Methods for Quadrotor UAV," *International Journal of Robotics and Control Systems*, vol. 2, no. 4, pp. 652-665, 2025, http://dx.doi.org/10.31763/ijrcs.v2i4.743.

[5] G. G. Garrido, O. J. Santos-Sánchez H. Romero-Trejo, O. García-Pérez, "Discrete integral optimal controller for quadrotorattitude stabilization: Experimental results," *Applied Sciences*, vol. 13, no. 16, p. 9293, 2023, https://doi.org/10.3390/app13169293.

[6] M. Ghanifar, M. Kamzan, M. Tayefi, "Different intelligent methods for coefficient tuning of quadrotor feedback linearization controller," *Journal of Aerospace Science and Technology*, vol. 16, no. 1, pp. 56-65, 2023, https://doi.org/10.22034/jast.2023.355914.1123.

[7] M. Karahan, C. Kasnakoglu, A. N. Akay, “Robust backstepping control of a quadrotor uav under pink noise and sinusoidal disturbance,” *Studies in Informatics and Control*, vol. 32, no. 2, pp. 15-24, 2023, https://doi.org/10.24846/v32i2y202302.

[8] A. Gün, “Attitude control of a quadrotor using pid controller based on differential evolution algorithm,” *Expert Systems with Applications*, vol. 229, p. 120518, 2023, https://doi.org/10.1016/j.eswa.2023.120518.

[9] M. Idrissi, M. Salami, F. Annaz, “A review of quadrotor unmanned aerial vehicles: Applications, architectural design and control algorithms,” *Journal of Intelligent & Robotic Systems*, vol. 104, no. 22, pp. 1-33, 2022, https://doi.org/10.1007/s10846-021-01527-7.

[10] H. Asharioun, M. Jahanshahifar, E. Davoudi, M. Mazare, “Real-time fault tolerant attitude stabilization control of a quadrotor in the presence of actuator fault,” *Journal of Modares Mechanical Engineering*, vol. 23, no. 7, pp. 424-437, 2023, https://doi.org/10.22034/mme.23.7.424.

[11] B. Liu, Y. Wang, O. Mofid, S. Mobayen and M. H. Khooban, "Barrier Function-Based Backstepping Fractional-Order Sliding Mode Control for Quad-Rotor Unmanned Aerial Vehicle Under External Disturbances," *IEEE Transactions on Aerospace and Electronic Systems*, vol. 60, no. 1, pp. 716-728, 2024, https://doi.org/10.1109/TAES.2023.3328801.

[12] A. Ruiz, D. Rotondo, B. Morcego, “Design of shifting state-feedback controllers for constrained feedback linearized systems: Application to quadrotor attitude control,” *International Journal of Robust and Nonlinear Control*, vol. 34, no. 4, pp. 2614-2638, 2023, https://doi.org/10.1002/rnc.7098.

[13] A. -W. A. Saif, K. B. Gaufan, S. El-Ferik and M. Al-Dhaifallah, "Fractional Order Sliding Mode Control of Quadrotor Based on Fractional Order Model," *IEEE Access*, vol. 11, pp. 79823-79837, 2023, https://doi.org/10.1109/ACCESS.2023.3296644.

[14] Z. Yasmine, B. Karim, B. Razika, B. Younes, “Adaptive Fuzzy Logic Control of Quadrotor,” *International Journal of Robotics and Control Systems*, vol. 4, no. 4, pp. 2095-2118, 2024, http://dx.doi.org/10.31763/ijrcs.v4i4.1583.

[15] A. Noordin, M. A. Basri, Z. Mohamed, “Real-time implementation of an adaptive pid controller for the quadrotor mav embedded flight control system,” *Aerospace*, vol. 10, no. 1, p. 59, 2023, https://doi.org/10.3390/aerospace10010059.

[16] T. Zhao, W. Li, “Lqr-based attitude controllers design for a 3-dof helicopter system with comparative experimental tests,” *International Journal of Dynamics and Control*, vol. 12, pp. 1063-1072, 2024, https://doi.org/10.1007/s40435-023-01242-1.

[17] D. Wang, Q. Pan, Y. Shi, J. Hu and C. Zhao, "Efficient Nonlinear Model Predictive Control for Quadrotor Trajectory Tracking: Algorithms and Experiment," *IEEE Transactions on Cybernetics*, vol. 51, no. 10, pp. 5057-5068, 2021, https://doi.org/10.1109/TCYB.2020.3043361.

[18] N. Basil, B. M. Sabbar, H. M. Marhoon, A. F. Mohammed, A. Ma'arif, “Systematic Review of Unmanned Aerial Vehicles Control: Challenges, Solutions, and Meta-Heuristic Optimization,” *International Journal of Robotics and Control Systems*, vol. 4, no. 4, pp. 1794-1818, 2024, https://doi.org/10.31763/ijrcs.v4i4.1596.

[19] A. M.A. Abitha, A. Saleem, “Quadrotor Modeling Approaches and Trajectory Tracking Control Algorithms: A Review,” *International Journal of Robotics and Control Systems*, vol. 4, no. 1, pp. 401-426, 2024, https://doi.org/10.31763/ijrcs.v4i1.1324.

[20] Z. Bellahcen, M. Bouhamid, M. Denai, K. Asali, “Adaptive neural network-based robust H_∞ trackingcontrol of a quadrotor uav under wind disturbances,” *International Journal of Automation and Control*, vol. 15, no. 1, pp. 28-57, 2020, https://doi.org/10.1504/IJAAC.2021.111747.

[21] M. Elhesasy *et al*., “Non-linear model predictive control using casadi packagefor trajectory tracking of quadrotor,” *Energies*, vol. 16, no. 5, p. 2143, 2023, https://doi.org/10.3390/en16052143.

[22] K. Zhang, Y. Shi and H. Sheng, "Robust Nonlinear Model Predictive Control Based Visual Servoing of Quadrotor UAVs," *IEEE/ASME Transactions on Mechatronics*, vol. 26, no. 2, pp. 700-708, 2021, https://doi.org/10.1109/TMECH.2021.3053267.

[23] X. Zheng, X. Yang, H. Zhao and Y. Chen, "Saturated Adaptive-Law-Based Backstepping and Its Applications to a Quadrotor Hover," *IEEE Transactions on Industrial Electronics*, vol. 69, no. 12, pp. 13473-13482, 2022, https://doi.org/10.1109/TIE.2021.3139235.

[24] N. Basil, H. M. Marhoon, D. F. Sahib, A. F. Mohammed, H. M. Ridha, A. Ma'arif , "Accelerated black hole optimization algorithm with enhanced FOPID controller for omni-wheel drive mobile robot system," *Neural Computing and Applications*, vol. 37, pp. 16983-17014, 2025, https://doi.org/10.1007/s00521-025-11310-6.

[25] N. Basil *et al*., "Multi-criteria decision model for multicircular flight control of unmanned aerial vehicles through a hybrid approach," *Scientific Reports*, vol. 15, no. 18962, pp. 1-31, 2025, https://doi.org/10.1038/s41598-025-01508-y.

[26] M. G. M. Abdolrasol *et al*., "Artificial neural networks based optimization techniques: A review," *Electronics*, vol. 10, no. 21, p. 2689, 2021, https://doi.org/10.3390/electronics10212689.

[27] M. Maaruf, W. M. Hamanah, M. A. Abido, "Hybrid backstepping control of a quadrotor using a radial basis function neural network," *Mathematics*, vol. 11, no. 4, p. 991, 2023, https://doi.org/10.3390/math11040991.

[28] M. Wang, B. Chen and C. Lin, "Fixed-TimeBackstepping Control of Quadrotor Trajectory Tracking Based On Neural Network," *IEEE Access*, vol. 8, pp. 177092-177099, 2020, https://doi.org/10.1109/ACCESS.2020.3027052.

[29] F. S. Shahar, M. T. Hameed Sultan, M. Nowakowski, A. Łukaszewicz, "UGV UAV Integration Advancements for Coordinated Missions: A Review," *Journal of Intelligent & Robotic Systems*, vol. 111, no. 69, pp. 1-34, 2025, https://doi.org/10.1007/s10846-025-02273-w.

[30] D. R. Guevara, A. F. Contreras, O. J. Villareal, "A qlpv-mpc control strategy for trajectory tracking of quadrotors," *Machines*, vol. 11, no. 7, p. 755, 2023, https://doi.org/10.3390/machines11070755.

[31] A. Kapnopoulos, C. Kazakidis, A. Alexandridis, "Quadrotor trajectory tracking based on backstepping control and radial basis function neural networks," *Results in Control and Optimization*, vol. 14, p. 100335, 2024, https://doi.org/10.1016/j.rico.2023.100335.

[32] J. Lin, Z. Miao, Y. Wang, G. Hu, X. Wang and H. Wang, "Error-State LQR Geofencing Tracking Control for Underactuated Quadrotor Systems," *IEEE/ASME Transactions on Mechatronics*, vol. 29, no. 2, pp. 1146-1157, 2024, https://doi.org/10.1109/TMECH.2023.3292893.

[33] Z. Yang, S. Yan, C. Ming, X. Wang, "Intelligent dynamic trajectory planning of uavs: Addressing unknown environments and intermittent target loss," *Drones*, vol. 8, no. 12, p. 721, 2024, https://doi.org/10.3390/drones8120721.

[34] N. Basil *et al*., "Performance analysis of hybrid optimization approach for UAV path planning control using FOPID-TID controller and HAOAROA algorithm," *Scientific Reports*, vol. 15, no. 4840, pp. 1-24, 2025, https://doi.org/10.1038/s41598-025-86803-4.

[35] O. Arifianto, M. Farhood, "Optimal control of a small fixed-wing uav about concatenated trajectories," *Control Engineering Practice*, vol. 40, pp. 113-132, 2015, https://doi.org/10.1016/j.conengprac.2015.03.007.

[36] S. Taamallah, X. Bombois, P. M. Van den Hof, "Trajectory planning and trajectory tracking for a small-scale helicopter in autorotation," *Control Engineering Practice*, vol. 58, pp. 88-106, 2017, https://doi.org/10.1016/j.conengprac.2016.08.009/.

[37] S. Rauniyar, S. Bhalla, D. Choi, D. Kim, "Ekf-slam for quadcopter using differential flatness-based lqr control," *Electronics*, vol. 12, no. 5, p. 1113, 2023, https://doi.org/10.3390/electronics12051113.

[38] B. A. Francis, "The linear multivariable regulator problem," *SIAM Journal on Control and Optimization*, vol. 15, no. 3, pp. 186-505, 1977, http://dx.doi.org/10.1137/0315033.

[39] J. O. Escobedo-Alva, E. C. García-Estrada, L. A. Páramo-Carranza, J. A. Meda-Campaña and R. Tapia-Herrera, "Theoretical Application of a Hybrid Observer on Altitude Tracking of Quadrotor Losing GPS Signal," *IEEE Access*, vol. 6, pp. 76900-76908, 2018, https://doi.org/10.1109/ACCESS.2018.2883596.

[40] N. Cox, L. Marconi and A. R. Teel, "Hybrid internal models for robust spline tracking," *2012 IEEE 51st IEEE Conference on Decision and Control (CDC)*, pp. 4877-4882, 2012, https://doi.org/10.1109/CDC.2012.6426043.

[41] K. Xie, Y. Zheng, W. Lan, X. Yu, "Adaptive optimal output regulation of unknown linear continuous-time systems by dynamic output feedback and value iteration," *Control Engineering Practice*, vol. 141, p. 105675, 2023, https://doi.org/10.1016/j.automatica.2024.111601.

[42] G. Rousseau, C. S. Maniu, S. Tebbani, M. Babel, N. Martin, "Minimum-time b-spline trajectories with corridor constraints. Application to cinematographic quadrotor flight plans," *Control Engineering Practice*, vol. 89, pp. 190-203, 2019, https://doi.org/10.1016/j.conengprac.2019.05.022.

[43] J. P. Hespanha, "Linear Systems Theory," *Princeton University Press*, 2009, https://press.princeton.edu/books/hardcover/9780691179575/linear-systems-theory?srsltid=AfmBOorwOVttpVQQ53qrEz_fJoDHg2vt07vADRdN9m5Pw2wdqFmSTuFz.

[44] R. Goebel, R. G. Sanfelice and A. R. Teel, "Hybrid dynamical systems," *IEEE Control Systems Magazine*, vol. 29, no. 2, pp. 28-93, 2009, https://doi.org/10.1109/MCS.2008.931718.

[45] J. Hespanha, A. S. Morse, "Stability of switched systems with average dwell-time," *Proceedings of the 38th Conference on Decision and Control*, pp. 2655-2660, 1999, https://www.eng.yale.edu/controls/1999/average.pdf.

[46] R. Goebel, R. G. Sanfelice, A. R. Teel, "Hybrid Dynamical Systems. Modeling, Stability, and Robustness," *Princeton University Press*, 2012, https://books.google.co.id/books/about/Hybrid_Dynamical_Systems.html?id=JwrOY03fuGQC&redir_esc=y.

[47] L. A. Páramo-Carranza *et al*., "Discrete-time kalman filter for takagi–sugeno fuzzy models," *Evolving Systems*, vol. 8, no. 1, pp. 211-219, 2017, https://doi.org/10.1007/s12530-017-9181-0.

[48] J. A. Meda-Campaña *et al*., "On the rejection of random perturbations and the tracking of random references in a quadrotor," *Complexity*, vol. 2022, no. 1, pp. 1-16, 2022, https://doi.org/10.1155/2022/3981340.

[49] R. Velazquez-Sánchez, J. O. Escobedo-Alva, R. Peña-García, J. A. Meda-Campaña, "Identification of high-order nonlinear coupled systems using a data driven approach," *Applied Sciences*, vol. 14, no. 9, p. 3864, 2024, https://doi.org/10.3390/app14093864.

[50] M. Karahan, M. Inal, C. Kasnakoglu, "Fault Tolerant Super Twisting Sliding Mode Control of a Quadrotor UAV Using Control Allocation," *International Journal of Robotics and Control Systems*, vol. 3, no. 2, pp. 270-285, 2023, https://doi.org/10.31763/ijrcs.v3i2.994.

[51] M. Maaruf, M. S. Mahmoud, A. Ma'arif, "A Survey of Control Methods for Quadrotor UAV," *International Journal of Robotics and Control Systems*, vol. 2, no. 4, pp. pp. 652-665, 2022, https://doi.org/10.31763/ijrcs.v2i4.743.

[52] B. A. Francis, W. M. Wonham, "The internal model principle of control theory," *Automatica*, vol. 12, no. 5, pp. 457-465, 1976, https://doi.org/10.1016/0005-1098(76)90006-6.

[53] A. Lastra, "Parametric Geometry of Curves and Surfaces," *Birkhauser Cham*, 2021, https://doi.org/10.1007/978-3-030-81317-8.

[54] A. Isidori and C. I. Byrnes, "Output regulation of nonlinear systems," *IEEE Transactions on Automatic Control*, vol. 35, no. 2, pp. 131-140, 1990, https://doi.org/10.1109/9.45168.

[55] N. H. Sahrir, M. A. Basri, "PSO–PID Controller for Quadcopter UAV: Index Performance Comparison," *Arabian Journal for Science and Engineering*, vol. 48, pp. 15241-15255, 2023, https://doi.org/10.1007/s13369-023-08088-x.

[56] Z. Qin, "PID Control Algorithm Based on Particle Swarm Optimization for Quadrotor UAV with Tip Defect," *Academic Journal of Science and Technology*, vol. 7, no. 2, pp. 101-105, 2023, https://doi.org/10.54097/ajst.v7i2.11951.

[57] B. E. Demir, F. Demir, "Comparison of metaheuristic optimization algorithms for quadrotor pid controllers," *Tehnicki vjesnik*, vol. 30, no. 4, pp. 1096-1103, 2023, https://doi.org/10.17559/TV-20221108150435.

[58] A. Ghasemi, M. A. Azimi, "Adaptive fuzzy pid control based on nonlinear disturbance observer for quadrotor," *Journal of Vibration and Control*, vol. 29, no. 13-14, pp. 2965-2977, 2022, https://doi.org/10.1177/10775463221089734.

[59] C. B. Jabeur, H. Seddik, "Optimized neural networks pid controller with wind rejection strategy fora quad-rotor," *Journal of Robotics and Control*, vol. 3, no. 1, pp. 62-72, 2022, https://doi.org/10.18196/jrc.v3i1.11660.

[60] C. Zhang, J. Li, Z. Gao, "Attitude control of quadrotor uav based on fuzzy PID control under small disturbance," *Highlights in Science, Engineering and Technology*, vol. 53, pp. 199-207, 2023, https://doi.org/10.54097/hset.v53i.9725.